Examples of Applications of Electrophysiology

All the techniques that we have discussed, flux measurements, steady-state and transient current measurements, as well as single-channel recordings and the corresponding analysis can be applied to the analysis of structure-function relationships. Such structure-function information can be obtained if we characterize and compare the function of wild-type and chemically or genetically modified transporters by using these techniques. The latter also includes naturally occurring mutations that are the source of various diseases; this is an important feature for the understanding and curing of such diseases.

For many of the transporters the amino acid sequence and the possible orientation of the protein in the membrane, or even the three-dimensional structures have been determined. In the following, we will illustrate the strategy of an electrophysiologist in investigating structure, function and regulation of membrane transport using as an example the Na^+,K^+-ATPase (◘ Fig. 8.1), the neurotransmitter transporter GAT (Na^+-dependent GABA transporter; ◘ Fig. 8.4; ► Sect. 8.1), and the nucleotide receptors (◘ Fig. 8.6) that form channels in the presence of extracellular ATP (► Sect. 8.2).

For an understanding of drug action as well as the development of new drugs for the treatment of diseases, electrophysiology is a powerful method to elucidate drug receptor interaction. As an example, this will be illustrated for viral ion channels (► Sect. 8.3) that are essential for virus reproduction.

8.1   Structure-Function Relationships of Carrier Proteins

8.1.1   The Na^+,K^+-ATPase

The Na^+,K^+-ATPase (for a review, see [Vasilets and Schwarz 1993]) is a heterodimer composed of an α subunit of about $100\,kDa$ and a smaller glycosylated β subunit of about $60\,kDa$ (see ◘ Fig. 8.1). At least four isoforms of the $α$ subunit have been identified, and three isoforms of the $ß$ subunit that all show tissue-specific distribution. The $α$ subunits host all functionally significant sites including ATP-binding and phosphorylation sites, the sites for interaction with the transported cations and for specific inhibitors like cardiotonic steroids, and the binding site for palytoxin (see ► Sect. 7.2).

Measurements of the electrogenic current generated by the Na^+,K^+ pump confirm that mutation of Q_{118} and N_{129} to the charged residues R and D, respectively, causes insensitivity of the ATPase to the cardiac glycoside Ouabain. The $ß$ subunit is necessary for proper folding of the $α$ subunit and for assembly and proper insertion of the entire protein into the cell membrane. The combination of an $α$ subunit with different $ß$ subunits results in a different function and, therefore, a regulatory role of the $ß$ subunit has been discussed. In addition, a γ subunit has been identified, which also seems to have a regulatory function. One option to monitor modulation of the ion transport is the measurement of a pump-mediated current under voltage clamp.

In the $α$ subunit of the Na^+,K^+-ATPase several negatively charged amino acids can be localized in intramembraneous domains (◘ Fig. 8.1) that may be involved in interaction with the transported cations. Mutation of some of these amino acids to Ala indeed alters the apparent dielectric length of the access channel that is represented by the effective valencies z (see, e. g. glutamate 334 and 960 in ◘ Fig. 8.2).

The N-terminus is the area, which shows the highest degree of diversity among the different isoforms of the $α$ subunits, and may, therefore, account for isoform-specific function in different tissue. In fact, mutations (like truncation as illustrated in ◘ Fig. 8.2) or chemical modifications
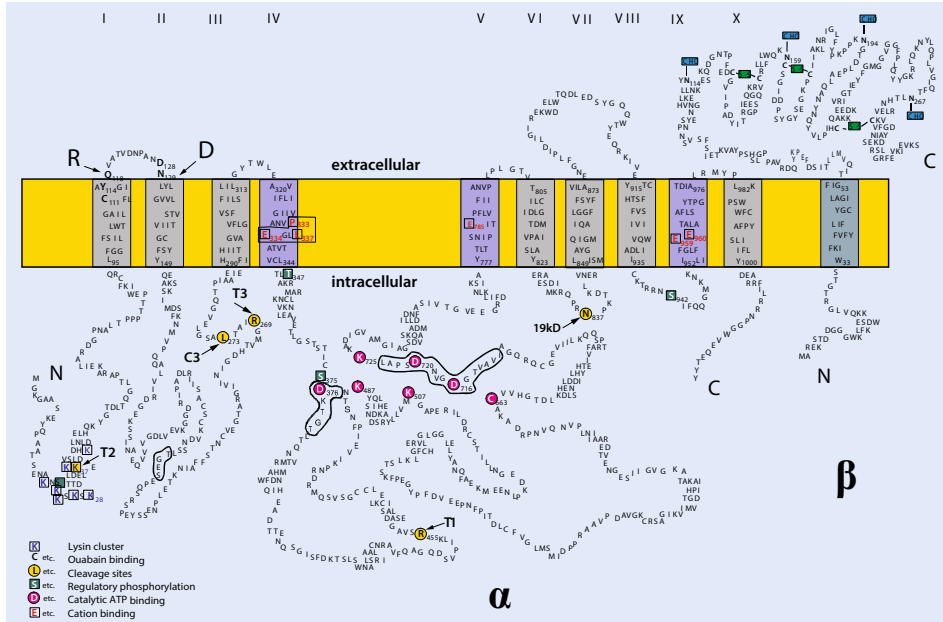
Fig. 8.1 Amino acid sequence of the Na$^+$,K$^+$ ATPase. (Based on Vasilets and Schwarz 1993)
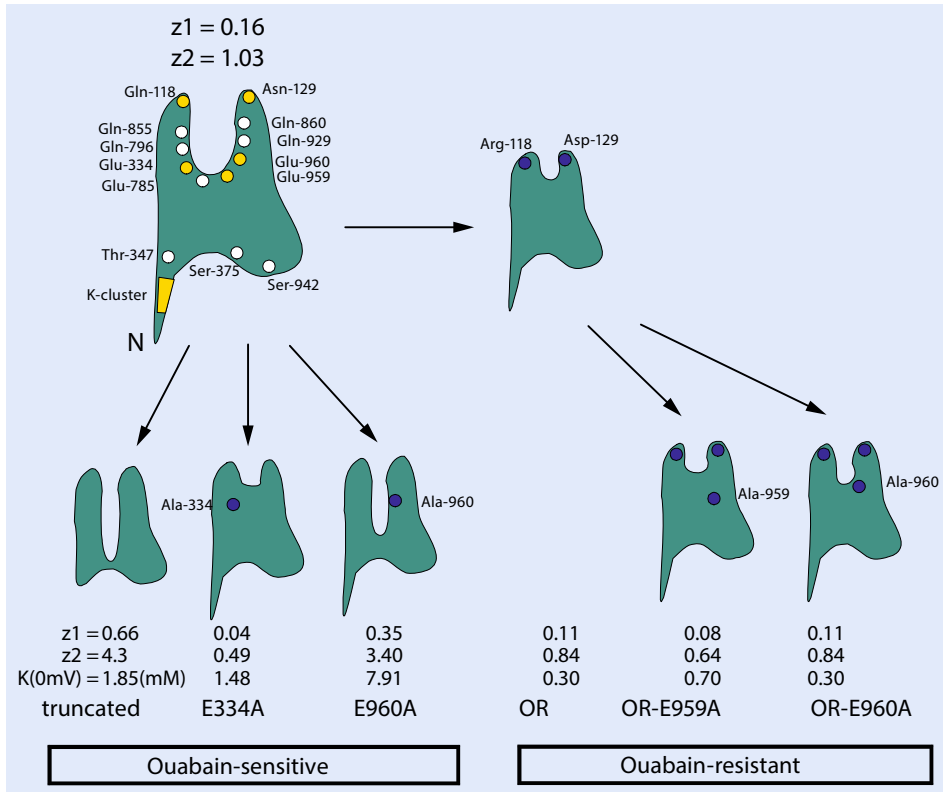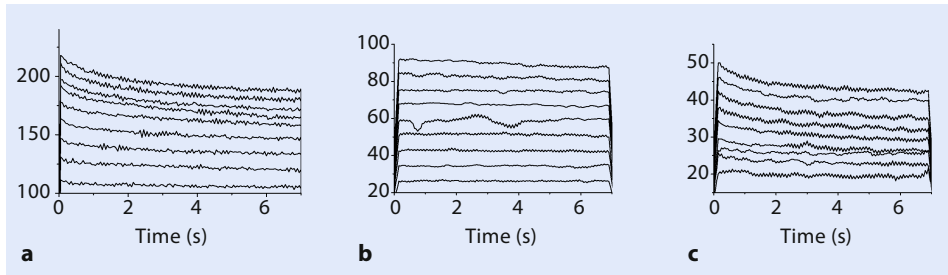

Fig. 8.2 "Dentist's" presentation of the Na$^+$,K$^+$-ATPase

Fig. 8.3a,b PTX-induced current in wild-type (**a**) and truncated mutants (**b**) without N-terminal peptide, (**c**) with the peptide added to the internal solution (based on Wu et al. 2003)

(by, e.g. regulatory phosphorylation, see ■ Fig. 8.1) within the N-terminus leads to altered transport function including external cation interaction and external binding of the specific inhibitor Ouabain. It is interesting to mention that the highly flexible, cytoplasmic N-terminus interferes with the external interactions. This finding is an example illustrating the allosteric interaction within the complex protein structure.

We have described above (▶ Sect. 7.2) that palytoxin transfers the Na^+,K^+ pump into a channel. During long-lasting voltage-clamp pulses the palytoxin-induced current inactivates at very positive potentials (■ Fig. 8.3a).

Inactivation at positive potentials of Na^+ and K^+ channels has been ascribed to a positively charged ball at the N-terminus blocking the internal channel mouth (bal at a chain), which leads to an inward-rectifying steady-state IV relationship (cf., e.g. also ▶ Sect. 5.2.2). A similar interpretation has been suggested for the PTX-modified Na^+,K^+ pump. Indeed, the truncated mutant does not show inactivation anymore (■ Fig. 8.3b), while application of the truncated N-terminal peptide restores inactivation (■ Fig. 8.3c).

8.1.2   The Na-Dependent GABA Transporter (GAT1)

The activity of neurotransmitter transporters plays an important role in termination of synaptic transmission. Therefore, a detailed knowledge of structure-function relationships is essential for understanding the physiology, pathophysiology and pharmacology of brain function. We have already mentioned the importance of regulatory phosphorylation of the Na^+,K^+ pump by protein kinases, and this is also the case for neurotransmitter transporters. The strategy for identification of such sites is the same as described for the Na^+,K^+ pump. Possible candidates for phosphorylation of GAT1 (see ■ Fig. 8.4) have been mutated; the mutants are then functionally characterized and compared with the wild-type transporter. Again, transporter-mediated current can serve as a measure for transport activity.

More recently, also glycosylation has been proposed to be involved in regulation of the transport function. Mutations in the glycosylation sites (see N_{176}, N_{181}, N_{184} in ■ Fig. 8.4) indeed lead to altered transport. The example illustrated in ■ Fig. 8.5 shows that mutation of two of the three asparagines (N) to aspartic acid (D) leads to reduced sensitivity for extracellular Na^+.
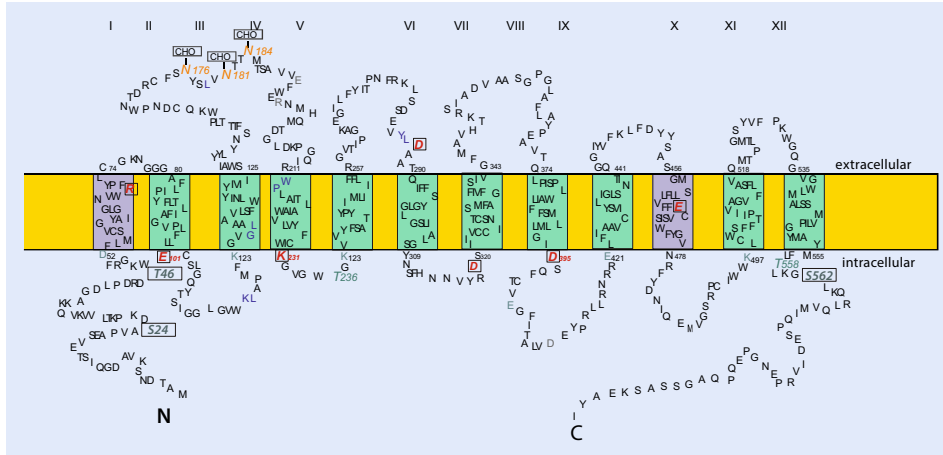
Fig. 8.4 Amino acid sequence of mouse GAT1

Fig. 8.5 Effect of mutation of glycosylation sites (based on Liu et al. 1998). The code letter for amino acids represent positions 176, 181 and 184
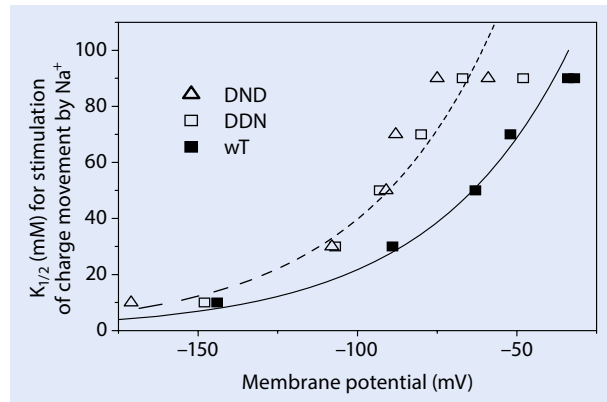
8.2 Structure-Function Relationships of Ion Channels

Ion channels are classified due to their diverse modes of function or molecular structure. This can be ion selectivity, modes of gating, number of subunits comprising the functional channel, number of transmembrane domains or sequence homologies. Classically, ion channels are divided into major families having important properties in common like gating mechanisms and ion selectivity. Some of the families will be briefly presented in the next paragraphs.

8.2.1 Families of Various Ion Channels

The Voltage-Gated Ion Channel (VIC) Superfamily

Although some members of this family are in addition controlled by ligand binding, their activity is generally controlled by the transmembrane electrical field. Functionally characterized members are selectively permeable for K^+, Na^+, or Ca^{2+} ions. Members of the VIC family play a role in the generation of action potentials and modulation of excitability of cells.

Fig. 8.6 Amino acid sequence of human P2X$_1$

The K$^+$ channels usually consist of homotetrameric structures with each subunit possessing six transmembrane domains (see also ■ Fig. 6.8). At least ten types of K$^+$ channels are known, each responding in different ways to different stimuli: voltage-sensitive (Ka, Kv, Kvr, Kvs and Ksr), Ca^{2+}-sensitive (BKCa, IKCa and SKCa) and receptor-coupled channels (KM and KACh). There are also tetrameric channels in which each subunit possesses two transmembrane (TM) domains that are homologous to TM-domains 5 and 6 of the six TM-domain types (inward rectifier Kir).

The α subunits of the Ca^{2+} and Na$^+$ channels are about four times as large as the K$^+$-channel subunits and possess four sequence repeats, with each repeat being homologous to the single subunit in the homotetrameric K$^+$ channels (compare ■ Fig. 6.8 and 6.11). There are five types of Ca^{2+} channels (L, N, P, Q and T), and at least six types of Na$^+$ channels (I, II, III, µ1, H1 and PN3).

The Ligand-Gated Ion Channel (LIC) Family

Members of the LIC family of ionotropic neurotransmitter receptors are activated by acetyl-choline, serotonin, glycine, glutamate or γ-aminobutyric acid (GABA). All of these receptor channels are homo- or heteromers of three, four or five subunits. The best characterized ones are the nicotinic acetylcholine receptors, which are pentameric channels of $\alpha_2\beta\gamma\delta$ subunit composition. Channels of the LIC family are selective for cations or anions (e.g. the acetylcholine receptors are cation-selective, while glycine receptors are anion-selective).

The Chloride Channel (ClC) Family

The large ClC family consists of dozens of sequenced proteins derived from bacteria, plants and animals. These proteins exhibit 10–12 putative transmembrane α-helical domains and appear to be present in the membrane as homodimers. While one member of the family, *Torpedo* ClC-O, has been reported to have two channels, one per subunit, others are believed to have just one. All functionally characterized members of the ClC family are permeable for Cl^-, some of them are voltage-dependent. These channels are involved in a variety of physiological functions (cell volume regulation, membrane potential stabilization, signal transduction, transepithelial transport, etc.). Different homologues exhibit different anion selectivities, i.e. ClC4 and ClC5 share an $NO_3^- > Cl^- > Br^- > I^-$ conductance sequence, while ClC3 has an $I^- > Cl^-$ selectivity. ClC4 and ClC5 channels exhibit outward rectifying currents with currents only at voltages more positive than +20 mV.

The Gap Junction-Forming (Connexin) Family

Gap junctions consist of clusters of closely packed pairs of transmembrane channels in adjacent cells, the connexons, through which small molecules diffuse between neighbouring cells. The connexons consist of homo- or heterohexameric arrays of connexins, and the connexon in one plasma membrane docks end-to-end with a connexon in the membrane of a closely opposed cell. Over 15 connexin subunit isoforms are known. They vary in size between about 25 and 60 kDa. They have four putative transmembrane α-helical domains. A dodecameric channel is formed by two hexamers, and therefore, consists of 48 transmembrane domains in total.

The Epithelial Na$^+$ Channel (ENaC) Family

The ENaC family consists of more than 20 sequenced proteins exclusively from animals. There exist voltage-insensitive ENaC homologues in the brain. Some of these proteins are involved in touch sensitivity; other members of the ENaC family, the acid-sensing Na$^+$ channels (H$^+$-gated), ASIC1-3, mediate pain sensation in response to tissue acidosis. The (FMRF-amide)-activated Na$^+$ channel is the first peptide neurotransmitter-gated ionotropic receptor that was sequenced. All members of this family exhibit a topology with intracellular N- and C-termini, two transmembrane spanning segments, and a large extracellular loop. Three homologous ENaC subunits, α, β and γ, have been shown to assemble to form the highly Na$^+$-selective channel with the stoichiometry $\alpha\beta\gamma$ in a heterotrimeric architecture.

Mechanosensitive Ion Channels

Another interesting group of ion channels are those that are gated by mechanical stress, allowing transduction of mechanical forces into electrical signals (see, e.g. Delmas and Coste 2013; Ranade et al. 2015). In particular, the patch-clamp technique of applying mechanical or osmotic stress to a cell and recording electrical responses reveals a continuously growing number of mechanosensitive or stretch-activated (SAC) ion channels (Nilius and Honoré 2012). A class of mechanosensitive channels that was conserved throughout evolution is formed by the Piezo

channels (Bagriantsev et al. 2014). Another large class of ion channels sensitive to physical stimuli is formed by the transient receptor potential (TRP) channels (Christensen and Corey 2007).

Mechanosensitive channels are involved in all kinds of mechanosensation, including, e. g. touch sensation, hearing or regulation of the tone of smooth muscle fibres. The transfer from an open to a closed configuration can be governed by mechanical forces on the membrane protein via the lipid bilayer or via tethered cytoskeletal or extracellular structures.

8.2.2   ATP-Gated Cation Channel (ACC) Family

In the following, we will present the strategy how electrophysiology can be utilized to learn about structure-function relationships of ion channels. As an example, we will use ATP-gated ion channels and focus on members of the P2X receptor family.

Structure and Classification of P2X Receptors

The relatively new class of ATP-gated ion channels, which belongs to the group of ligand-gated ion channels, will be described in more detail since, we will use members of this group as our last example for application of electrophysiological techniques in analysis of structure-function relationships.

Because the common feature of these channels is the sensitivity to extracellular ATP, they are termed nucleotide receptors. Another commonly used name is P2X receptors, and formerly they were known under the name purinoceptors. Although it was already proposed in 1972 that ATP plays a functional role as a neurotransmitter, it took until 1994 for the first two isoforms $P2X_1$ and $P2X_2$ to be cloned from rat vas deferens and PC12 cells, respectively.

From hydropathy analysis, a now commonly accepted secondary structure with intracellular N- and C-termini, a large extracellular loop and two transmembrane domains were derived (see ◘ Fig. 8.6), which resemble the architecture of the ENaC family. As is also known from other ion channel proteins, the functional channel unit is composed of more than one subunit. A quaternary structure of three subunits forming the functional receptor has been published (Nicke et al. 1998); a stoichiometry that is different from what is known for other ligand-gated ion channels that are usually composed from tetramers or pentamers.

Nowadays, seven isoforms (◘ Table 8.1) and various splice variants are known, which have more or less different pharmacological and functional properties (Burnstock 1999). Since all of the seven isoforms are ionotropic ion channels (meaning that receptor and channel function are localized on the same protein multimer), electrophysiology is the method of choice to characterize their functional properties.

Before we introduce some of the electrophysiological data obtained for the $P2X_1$ and $P2X_2$ receptor, we give a short overview of the most evident differences between the subtypes. Although extracellular ATP is able to activate each of the ATP receptors, the ATP derivative α-ß-methylene-ATP is an agonist only for $P2X_1$ and $P2X_3$. More or less pronounced desensitization is obtained for all P2X receptors subtypes, which means that the agonist induces an opening of the ion channels, but then channels close even in the presence of the agonist.

Fast inactivation within about a second has been found for $P2X_1$ and $P2X_3$, and slightly slower for the $P2X_4$ receptors, whereas the other subtypes desensitize only slowly and incompletely. A special feature of the $P2X_7$ receptor is the formation of a large pore with a diameter of 3–5 nm after prolonged application of the agonist. Similar behaviour, where at least the ion selectivity changes after prolonged activation, is also discussed for the other subtypes.

Table 8.1 Comparison of the known P2X subtypes

	P2X$_1$	P2X$_2$	P2X$_3$	P2X$_4$	P2X$_5$	P2X$_6$	P2X$_7$
α-β-methylene-ATP	+	−	+	−	−	−	−
Desensitization	Fast & complete	Slow & incompl.	Fast & complete	Middle & incompl.	Slow & incompl.	Slow & incompl.	Slow & incompl.

Fig. 8.7 Current trace of the P2X$_1$ receptor in an outside-out oocyte-membrane patch at a holding potential of −60 mV with superimposition of several single-channel events
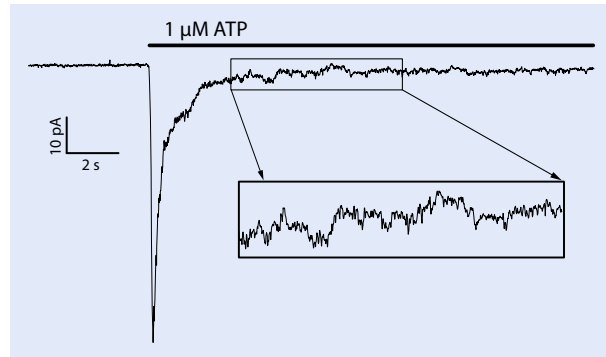
8.2.3 Experimental Results

In the following paragraphs we will present some results on the functional properties of the P2X$_1$, and P2X$_2$ receptor. Although analysis of single-channel activity can provide the most valuable insight into ion-channel characteristics, it is sometimes difficult to detect single channel events depending on single-channel conductance, gating behaviour and channel density. In the case of the P2X receptors, mainly macroscopic currents have been analyzed either due to fast desensitization (P2X$_1$ and P2X$_3$) or due to fast gating (flickering) of the P2X$_2$ receptors (Ding and Sachs 1999). ▪ Figure 8.7 shows a current trace of the P2X$_1$ receptor in an outside-out oocyte-membrane patch. It is only at the end of the trace that current fluctuations caused by the opening and closing of the channels can be resolved.

The data shown in the following were recorded by the two-electrode voltage-clamp (TEVC) technique (▶ Sect. 3.5.1 (*The Two-Microelectrode Voltage Clamp*)) with *Xenopus* oocytes (▶ Sect. 7.1.2). Therefore, the currents represent simultaneous activity of a huge number of ion channels (millions) leading to currents in the μA-range. *Xenopus* oocytes do not possess endogenous nucleotide receptors and are, therefore, an ideal tool for studying these channels after injection of the appropriate cRNAs.

Since P2X$_1$ and P2X$_3$ receptors show fast activation and desensitization (within 1 s), a fast and well-defined solution exchange is a prerequisite for correctly time-resolved measurements. Due to the large size of the oocyte (with a diameter of 1.2 mm) a fast solution exchange is not easy to achieve, but is possible with a special design: a solution exchange system where the oocyte is placed in a small oocyte chamber of about 10 μl volume in combination with fast perfusion (200 μl/s). This design allows an exchange time (5–95 %) in the range of 100–200 ms. This can be determined, for example, by activating expressed nicotinic acetylcholine receptors with 30 μM acetylcholine (ACh) or by monitoring the current change induced by a concentration change from Na$^+$-rich to Na$^+$-deficient solution (▪ Fig. 8.8). The reproducibility of the solution
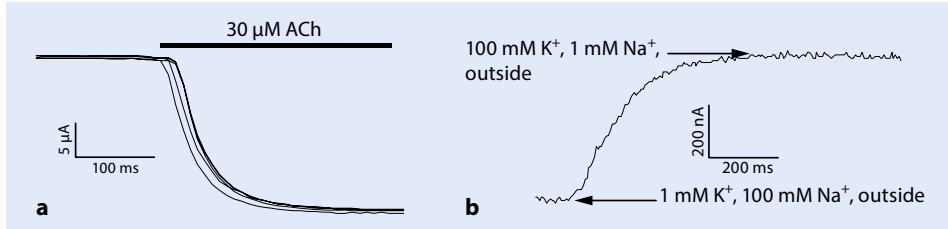
🔲 **Fig. 8.8a,b** Time course of solution exchange with nAChR-mediated currents (**a**) and with endogenous Na^+ conductance of the oocytes (**b**)

change is obvious in 🔲 Fig. 8.8(a) where seven consecutive responses to application of ACh at 1 min intervals are shown.

Although the exchange time of 100–200 ms is fast with respect to the large size of the oocyte, one should keep in mind that the currents that are elicited by a solution exchange (for example, ATP application to P2X receptors) are greatly influenced by the concentration change that occurs during the first 200 ms. A significantly faster solution change in intact oocytes will be difficult to achieve, and if this becomes necessary, one has to use the cell-free patch-clamp method (► Sects. 3.6.1 and 3.6.2), which allows for exchange times even in the sub-millisecond range.
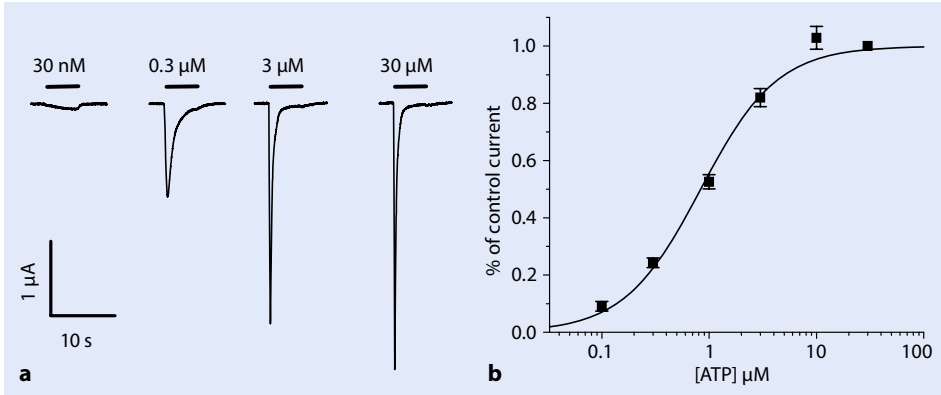
The P2X$_1$ Receptor

As already mentioned, the P2X$_1$ receptor is a fast desensitizing receptor that opens an intrinsic ion channel that is non-selectively permeable for small cations when challenged with extracellular ATP. 🔲 Figure 8.9 shows the current in response to 1 µM ATP for the first application of ATP (peak in 🔲 Fig. 8.9a) and for consecutive ATP applications at 5-minute intervals and a holding potential of −60 mV.

The receptor desensitizes in the presence of ATP completely within about 1 s. After a period of 5 min in ATP-free solution, typically only about 25 % of the initial receptor current can be restored. This means that desensitization is fast but the recovery from the desensitized state is slow. As a matter of fact, tens of minutes are necessary to restore the full initial current response. The response of the P2X$_1$ receptors is dependent on the extracellular ATP concentration with an EC$_{50}$ value (the concentration that is needed for half-maximum response) of about 1 µM.

🔲 Figure 8.10 shows a typical experiment for determination of the EC$_{50}$ value by activating the receptors with different ATP concentrations in the range 0.03–30 µM. 🔲 Figure 8.10b shows the dose-response curve of the receptor for ATP.
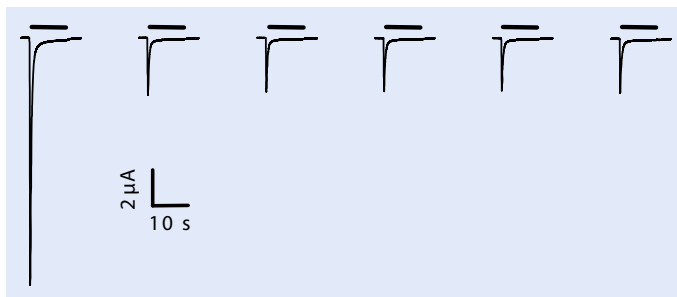
🔲 **Fig. 8.9** P2X$_1$ receptor currents activated with 1 µM ATP at 5 min intervals at a holding potential of −60 mV

Fig. 8.10a,b P2X$_1$ receptor currents activated with different ATP concentrations (**a**) and the ATP dose-response curve (**b**); EC$_{50}$ = 0.6 μM. Receptors were expressed in *Xenopus* oocytes after RNA-injection
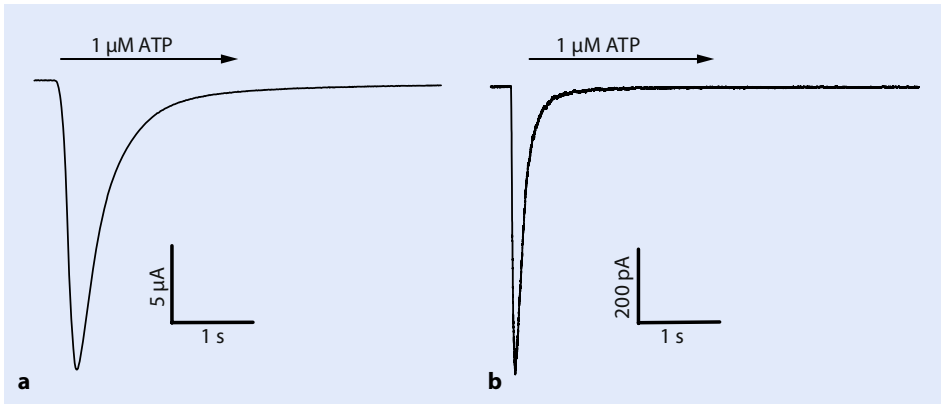

Fig. 8.11a,b Comparison of P2X$_1$-generated current activated by 1 μM ATP in TEVC (**a**) and an outside out macro-patch (**b**) at a holding potential of −60 mV

Since the P2X$_1$ receptor shows fast activation after application of extracellular ATP, it is interesting to compare the signals that can be measured with the TEVC and the patch-clamp method. Figure 8.11a shows the current trace from an intact oocyte Fig. 8.11b that from an excised outside-out patch. In both cases the channels are activated by 1 μM ATP.

This comparison demonstrates that onset as well as offset of the current are significantly different for both methods. This difference can be explained by the difference in speed of solution exchange that was complete within 2 ms by using the patch-clamp method, and hence two orders of magnitude faster than for the TEVC. Nevertheless, the TEVC method is commonly used, also for the analysis of fast receptor currents, but one should be careful with the quantitative interpretation of the data.

The P2X$_2$ Receptor

As an example for a nearly non-desensitizing P2X receptor we introduce the P2X$_2$ receptor, which, like all members of the P2X family, opens an intrinsic ion channel after extracellular application of an appropriate agonist. Analogous to the P2X$_1$ receptor, Fig. 8.12a shows P2X$_2$
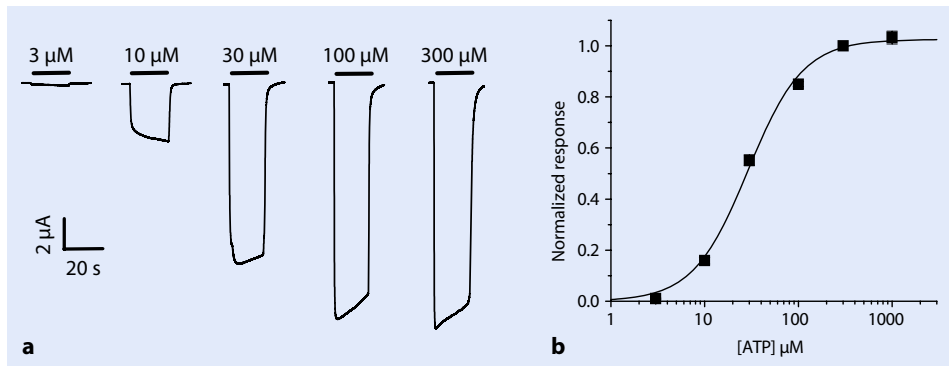
■ **Fig. 8.12a,b** P2X$_2$ receptor currents activated with different ATP concentrations (**a**) and the ATP dose-response curve (**b**); EC$_{50}$ = 29 µM, *HP* = −60 mV

currents activated by different ATP concentrations and ■ Fig. 8.12b the corresponding dose-response curve with an EC$_{50}$ value of about 30 µM.

After the presentation of these pharmacological data we will concentrate in the following on the use of electrophysiology in combination with biochemical methods. This combination can give answers to questions concerning the functional consequences of structural changes in the channel protein.

Analysis of the amino-acid sequence of the P2X$_1$ receptor revealed the presence of five consensus sequences for putative glycosylation localized on the extracellular loop of the protein (N1–N5, see ■ Fig. 8.6). Biochemical analysis of the receptor protein (expressed in oocytes) demonstrated that four out of these five sites are used for glycosylation. A question that cannot be answered with biochemical methods is whether functional properties of the expressed receptors (ATP dependence, kinetic parameters, etc.) are changed. Therefore, different constructs at which one or several glycosylation sites were removed by mutation of single amino acids were characterized electrophysiologically in respect to their ATP dependency and the magnitude of the ATP-activated current.

The electrophysiological analysis showed that removal of the third N-glycosylation site alters the apparent affinity of the receptor for ATP by a factor of about 3. None of the other N-glycosylation sites seem to have any influence on the ATP sensitivity. ■ Figure 8.13 gives a graphical representation of these results.

Taken together, results from the combination of molecular biology, biochemistry, and electrophysiology demonstrate that an increased number of missing glycosylation sites lead to a decrease in the surface appearance of the receptors (reflected by decreasing currents and the decreasing intensity of bands on the SDS-gel). A functional difference was only found for the constructs that were deficient of the third glycosylation site. These constructs showed the effect of decreased ATP sensitivity with an EC$_{50}$ value of 2 µM compared to the wild-type receptor with an EC$_{50}$ value of 0.6 µM.

8.3   Viral Ion Channels

In this section, we will present the strategy how electrophysiology can be combined with virology and pharmacology to develop new drugs against viral infection. As example, we will use the viral ion channels as a target for antiviral drugs. An interesting source for the development
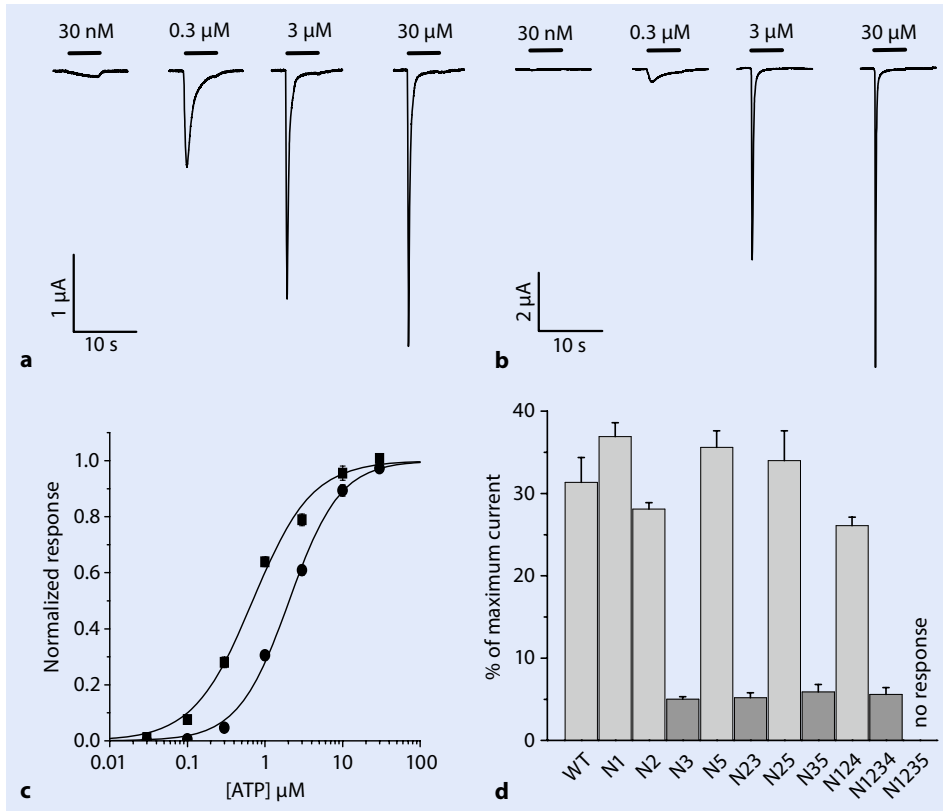
□ **Fig. 8.13a–d** P2X$_1$ receptor currents of wild-type (**a**), N3-mutated subunits activated by different ATP-concentrations (**b**), ATP dose-response curves for wild-type and mutant ΔN3, respectively (**c**). The bar graph shows the amount of current measured at 0.3 μM relative to the maximal current at 30 μM; it demonstrates that all mutants lacking the N-glycan at position N3 exhibit lower affinity for ATP (**d**)

of new medicines are drug components of traditional Chinese herbs. The finding of artemisinin extracted from *Artemisia annua* as an effective antimalarial drug by the Chinese scientist Youyou Tu (see Tu 2011) was honoured by the Nobel Prize in 2015. As a pharmacological tool, our focus will also be on drugs extracted from Chinese herbs.

The genomes of various viruses encode for proteins that may form ion-selective channels in the infected cell. These ion channels play important roles in the viral life cycle, and therefore, may represent a target for new antiviral drugs.

□ Table 8.2 lists examples of such channels (see, also Wang et al. 2011; Krüger and Fischer 2009; Fischer and Sansom 2002). The pores are formed by multi-homomers.

The viral life cycle involves a sequence of steps that actually may all form a target for antiviral drugs. As an example, □ Figure 8.14 illustrates various steps in the life cycle of coronavirus.

The virus attaches to the host cell, followed by incorporation of the virus, uncoating of the viral genome and replication processes with transcription and translation; finally, new viral particles are assembled, and the viruses are released from the host cell to infect new cells. In the case of coronavirus, the release is dependent on the activity of an ion channel, which is encoded by the viral genome and inserted into the membrane of the host cell. For SARS coronavirus

◻ **Table 8.2** Examples of viruses and their viral ion channels formed by multi-homomers, each subunit consists of 1–3 transmembrane segments (TMS)

| Virus family	Virus	Ion channel	Characteristics	Functional units
Coronaviridae	**SARS-CoV**	**3a**	**≈ 20 pS** **monovalent cation**	**Tetramer** **(3 TMS)**
Orthomyxovi-ridae	**Influenza A** **(swine flu)**	**M2**	**< fS** **proton**	**Tetramer** **(1 TMS)**
	Influenza B	BM2	< fS proton	Tetramer (1 TMS)
Picornaviridae	Poliovirus	2B	Non-selective	Tetramer (2 TMS)
Retroviridae	**HIV-1**	**Vpu**	**≈ 20 pS** **monovalent cation**	**Pentamer** **(1 TMS)**
Flaviviridae	HCV (hepatitis C)	p7	20–100 pS monovalent cation	Hexamer (2 TMS)
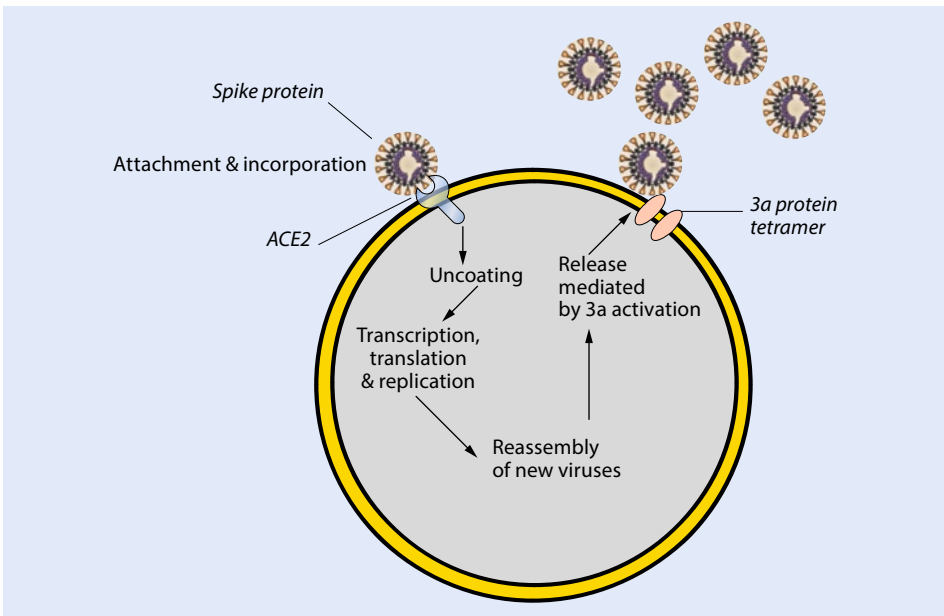
◻ **Fig. 8.14** Viral lifecycle of SARS CoV. Binding of viral spike protein with angiotensine-converting-enzyme-2 receptor of the host cell is followed by virus uptake, uncoating, and transcription and translation of the viral genome. After assembly of new viruses, 3a channel activity stimulates exocytotic release of the viruses from the host cell

(SARS CoV) the membrane protein is called 3a protein. Inhibition of any of these steps could represent a potential target for antiviral drugs.

In the following, we will illustrate how inhibition of ion-channel function can interfere with the viral life cycle. In ◻ Table 8.2 the respective viral ion channels dealt with in this section are printed in bold.

Fig. 8.15 Fluorescence-labelled 3a protein becomes visible in infected Vero E6 cells. (Based on Lu et al. 2006) (**a**). Orientation of 3a monomer in the cell membrane (**b**)
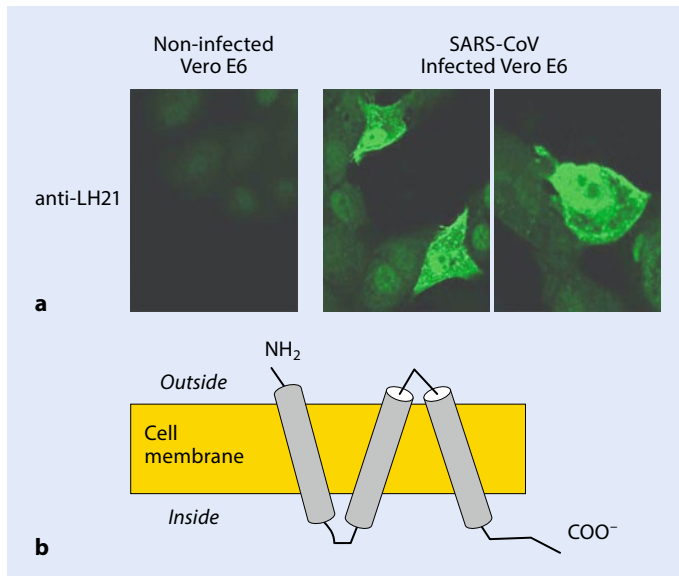
8.3.1 The 3a Protein of the Coronavirus

For the 3a protein of the SARS coronavirus (cf. ◘ Fig. 8.14) it was demonstrated (Lu et al. 2006) that tetramers form the ion channel that is incorporated into the membrane of the infected cell (see ◘ Fig. 8.15).

Patch-clamp analysis (◘ Fig. 8.16) revealed a single-channel conductance of about 20–30 pS. The channel is selectively permeable for monovalent cations with highest selectivity for K^+. As a result of 3a channel activity the membrane potential will depolarize, which results in Ca^{2+} channel activation. The increase in intracellular Ca^{2+} activity then facilitates the exocytotic release of viruses from the host cell (Lu et al. 2006).

Voltage clamping is an easy method to detect and analyze function of the viral ion channels. Again using the model system *Xenopus* oocyte as an expression system (cf. ▶ Sect. 7.1.2), drugs can be screened with respect to their interaction with the 3a protein. As a general rule, a method has to be elaborated that allows extracting the current component of interest from the total membrane current. Injection of cRNA for the 3a protein results in elevation of the membrane current that can be blocked by 10 mM Ba^{2+} in the extracellular medium (◘ Fig. 8.17).

Inhibition of 3a-Mediated Current by the Anthraquinone Emodin

During the SARS epidemic in 2003, herbal extracts were used in Asia to treat the disease supplementarily to treatment with western medicine. Among those were also extracts from *Rhei radix* (rhubarb), and an effective component seemed to be the phytodrug emodin (1,3,8-trihydroxy-6-methylanthracene-9,10-dione), which blocks the Ba^{2+}-sensitive current mediated by 3a protein, but not the endogenous component (◘ Fig. 8.18).

Emodin not only blocks 3a-mediated current, but with the same IC_{50} value of about 20 μM the number of viral RNA copies in the medium of infected cells (◘ Fig. 8.19a). The number of RNA copies correlates with the titre (◘ Fig. 8.19b) indicating that the RNA originates from intact viruses. This proves that emodin can act as an antiviral drug and may form the basis for the development of new drugs against coronavirus infection.
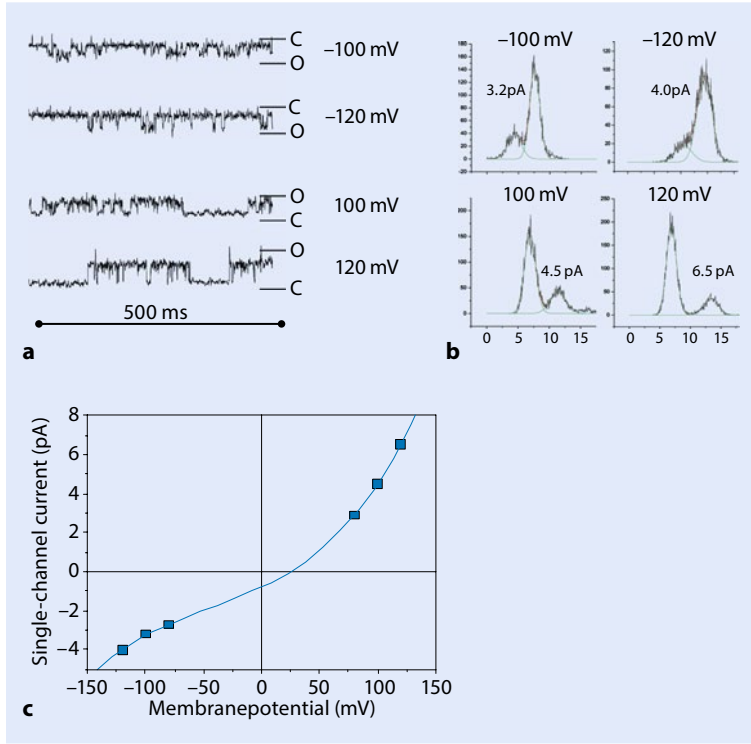
Fig. 8.16a–c Single-channel recordings from 3a protein expressed in *Xenopus* oocytes (**a**), histograms of the current amplitudes (**b**), and voltage dependence of the single-channel current (**c**) (based on Schwarz et al. 2012)
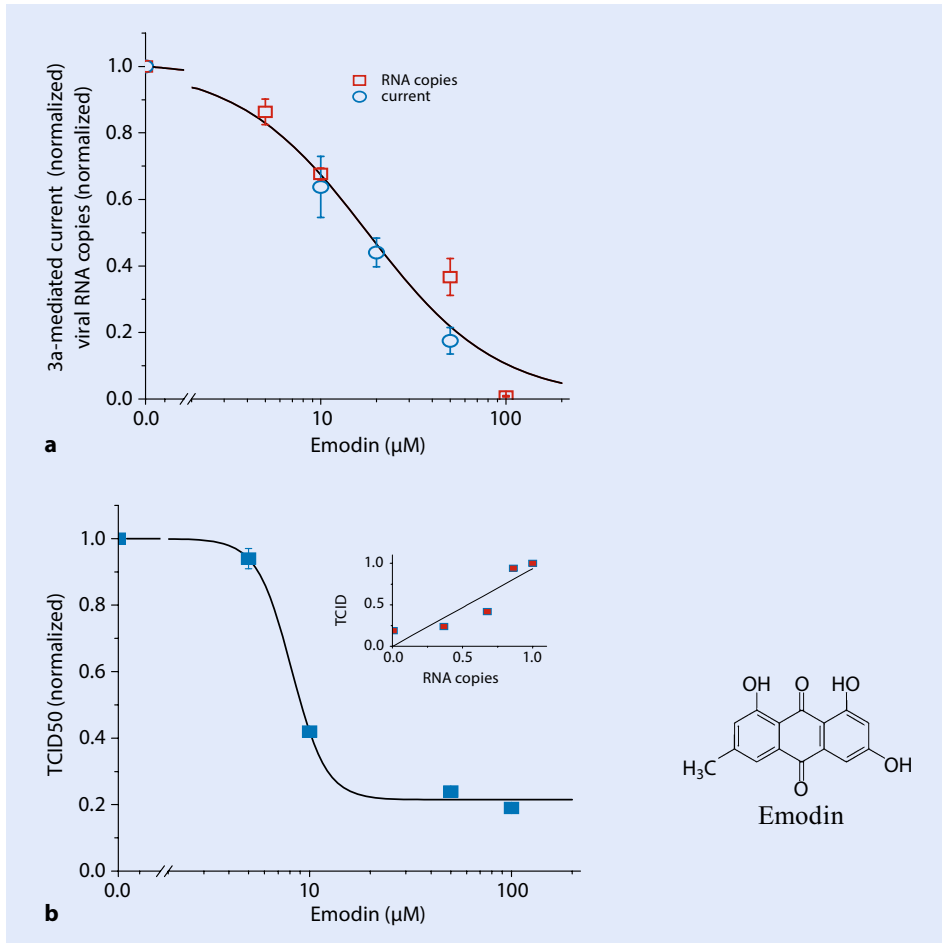
8
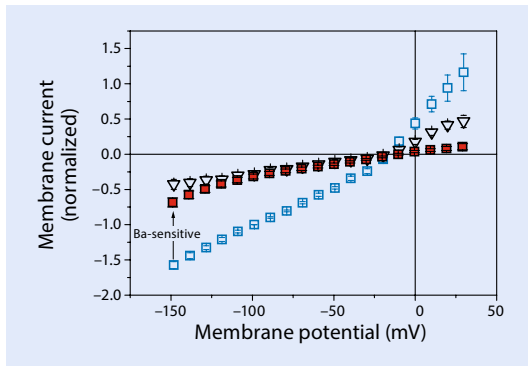
Fig. 8.17 Open triangles represent current-voltage dependency in oocytes not expressing 3a protein, open and filled squares those in 3a-expressing cells in the absence and presence of 10 mM Ba^{2+}, respectively. (Based on data from Lu et al. 2006)
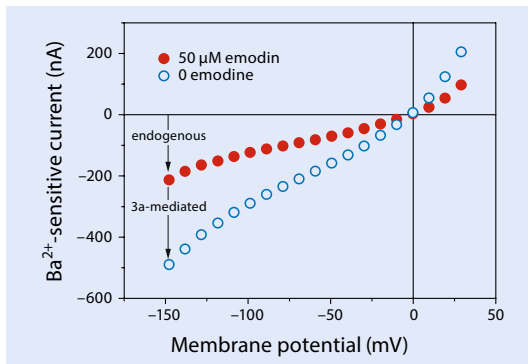
Fig. 8.18 Voltage dependency of Ba^{2+}-sensitive current in oocytes expressing 3a protein in the absence (*open circles*) and presence (*filled circles*) of 50 μM emodin, which completely inhibits 3a-mediated current but leaves endogenous component unaffected. (Based on Schwarz et al. 2011)
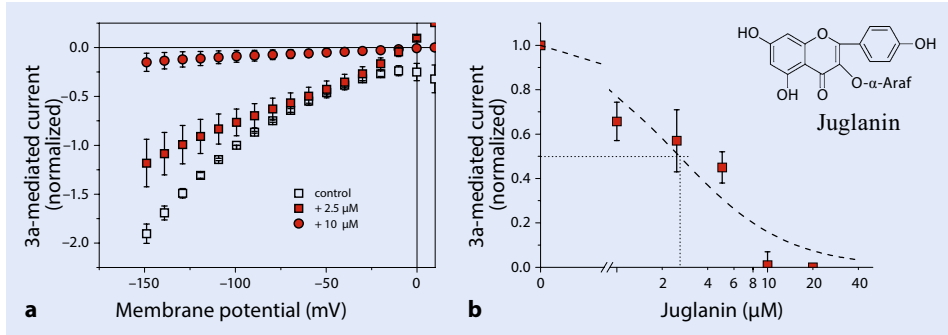
Inhibition of 3a-Mediated Current by the Kaempferol Glycoside Juglanin

Other effective phytodrugs are the flavonoids, especially kaempferol glycosides. The kaempferol glycoside juglanin effectively blocks 3a-mediated current (■ Fig. 8.20a), and it even more effective than emodin by an order of magnitude (IC$_{50}$ ≈ 2 μM) (■ Fig. 8.20b).

8.3.2   The Viral Protein Unit (Vpu) of HIV-1

The viral protein unit Vpu of HIV-1 is also a membrane protein but with only one transmembrane segment (■ Fig. 8.21a), and a channel permeable for monovalent cations is formed by a pentamer.

The activation of the channel is necessary for virus release (Schubert et al. 1996), and the search for Vpu channel blockers as antiviral drugs has been suggested. Vpu-mediated current can also be monitored as a Ba^{2+}-sensitive current (■ Fig. 8.21b) and can partially be blocked by the flavonoid genistein.

◘ Fig. 8.20a,b a Current-voltage dependencies of 3a-mediated current in *Xenopus* oocytes in the presence of different amounts of the kaempferol glycoside juglanin (inset in **b**). **b** Dependence of 3a-mediated current (at −60 mV) on juglanin concentration. (Based on Schwarz et al. 2014)
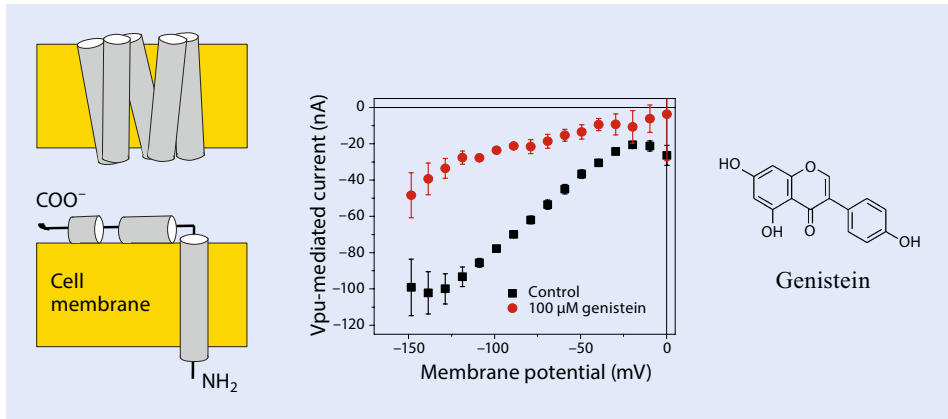

◘ Fig. 8.21a–c a Orientation of Vpu monomer in the membrane (*bottom*) and formation of ion channel by penta-mer (*top*). b Inhibition of Vpu-mediated current by 100 μM of the flavonoid genistein (**c**). (Based on Sauter et al. 2014)

8.3.3   The M2 (Matrix Protein 2) Protein of the Influenza A Virus

The genome of the influenza A virus (swine flu virus) encodes for an ion channel. As for the Vpu, this M2 protein has only a single transmembrane segment, but the channel is formed by a tetrameric structure (◘ Fig. 8.22a) that exhibits low conductance for protons. With decreasing pH, the M2-mediated current increases dramatically (◘ Fig. 8.22b). The activity of the channel also plays an essential role in virus production (see de Clercq 2006).

In contrast to the 3a protein, M2 is an integral membrane protein of the viron and is involved in the uncoating of the viruses by permitting passage of protons across the membrane of the viron. In previous times, one of the most effective inhibitors of M2 function was amantidine, and in the past, a potent medicine for treatment of influence A infection. Meanwhile, all influenza A viruses have become amantadine-resistant, and worldwide laboratories are searching intensively for substitutes.
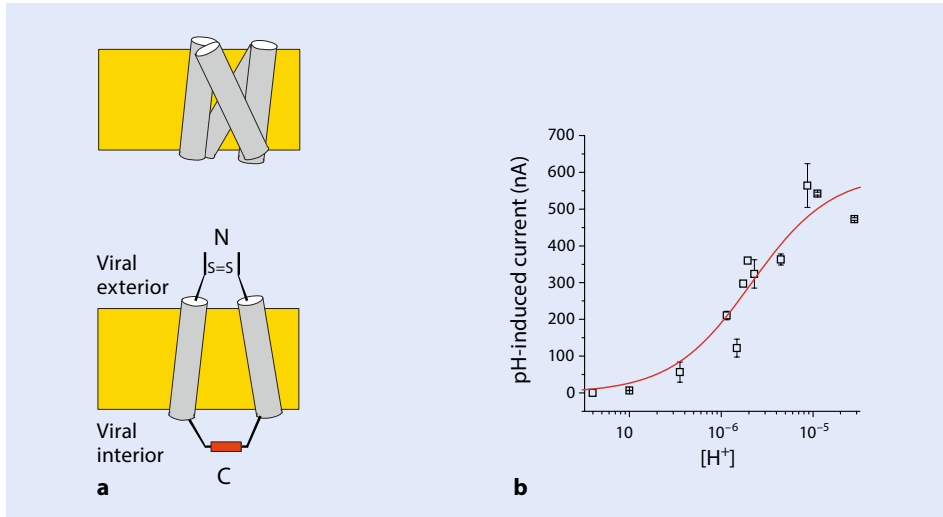
Fig. 8.22a,b a Illustration of structure of the M2 protein of the influenza A virus. *Lower part*: two monomers interacting with their N and C termini. *Upper part*: formation of the tetrameric channel. **b** pH dependency of current mediated by M2 protein expressed in *Xenopus* oocytes
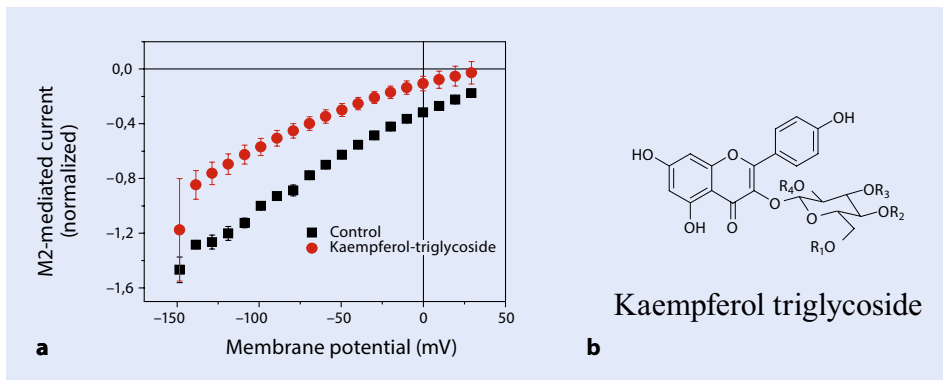
Fig. 8.23a,b Inhibition of M2-mediated current (**a**) by 20 µM kaempferol triglycoside (**b**)

Inhibition of M2-Mediated Current by Kaempferol Triglycosides

Kaempferol glycosides may also form the basis for new drugs against influenza A. A triglycoside has been found that effectively inhibits pH-sensitive current when M2 is expressed in *Xenopus* oocytes (Fig. 8.23).

In conclusion, the activity of various viral ion channels seems to be essential for virus reproduction in the infected cells. Hence, inhibition of channel activity by drugs will counteract that process, allowing the infected body to build up or strengthen its own immune system. Viral ion channels are, therefore, potential candidates for developing new antiviral drugs, and voltage clamping is an easy method to screen drugs, and detect and analyze inhibition of the ion channels. Screening of a large number of natural drugs revealed that kaempferol derivatives and anthraquinones may be interesting candidates.

Exercises

1. What are the major tasks of the sodium pump?
2. What are the functional meanings of the α-, β-, and γ-subunits of the sodium pump?
3. What is the physiological function of P2X receptors?
4. What role does a neurotransmitter transporter play in physiological and pathophysiological functions?
5. Which ion-channel families do you know?
6. Describe the role of viral ion channels in virus reproduction.
7. How can electrophysiology serve as a tool in development of antiviral drug? Name examples.

References

Bagriantsev SN, Gracheva EO, Gallagher PG (2014) Piezo proteins: Regulators of mechanosensation and other cellular processes. JBiolChem 289:31673–31681

Burnstock G (1999) Current status of purinergic signalling in the nervous system. Prog Brain Res 120:3–10

Christensen AP, Corey DP (2007) TRP channels in mechanosensation: direct or indirect activation. Nature RevNeurosc 8:510–521

De Clercq E (2006) Antiviral agents active against influenza A viruses. Nature RevDrug Discov 5:1015–1025

Delmas P, Coste B (2013) Mechano-gated ion channels in sensory systems. Cell 155:278–284

Ding S, Sachs F (1999) Single channel properties of P2X2 purinoceptors. J Gen Physiol 113:695–720

Eckstein-Ludwig U, Fei J, Schwarz W (1999) Inhibition of uptake, steady-state currents, and transient charge movements generated by the neuronal GABA transporter by various anticonvulsant drugs. Br J Pharmacol 128:92–102

Fischer WB, Sansom MSP (2002) Viral ion channels: structure and function. Biochim Biophys Acta 1561:27–45

Krüger J, Fischer WB (2009) Assembly of viral membrane proteins. J ChemTheory Comput 5(2009):2503–2513

Liu Y, Eckstein-Ludwig U, Fei J, Schwarz W (1998) Effect of mutation of glycosylation sites on the Na+ dependence of steady-state and transient current generated by the neuronal GABA transporter. Biochim Biophys Acta 1415:246–254

Lu W, Zheng BJ, Xu K, Schwarz W, Du LY, Wong CKL, Chen JD, Duan SM, Deubel V, Sun B (2006) Severe acute respiratory syndrome-associated coronavirus 3a protein forms an ion channel and modulates virus release. PNAS 103:12540–12545

Nicke A, Bäumert HG, Rettinger J, Eichele A, Lambrecht G, Mutschler E, Schmalzing G. (1998) P2X1 and P2X3 receptors form stable trimers: a novel structural motif of ligand-gated ion channels. EMBO J. 17(11):3016–3028

Nilius B, Honoré E (2012) Sensing pressure with ion channels. Trends Neurosci 35:477–486

Ranade SS, Syeda R, Patapoutian A (2015) Mechanically activated ion channels. Neuron 87:1162–1179

Rettinger J, Aschrafi A, Schmalzing G (2000) Roles of individual N-glycans for ATP potency and expression of the rat P2X1 receptor. J Biol Chem 275:33542–33547

Sauter D, Schwarz S, Wang K, Zhang RH, Sun B, Schwarz W (2014) Genistein as Antiviral Drug against HIV Ion Channel. Planta Med 80:682–687

Schubert U, Ferrer-Montiel AV, Oblatt-Montal M, Henklein P, Strebel K, Montal M (1996) Identification of an ion channel activity of the Vpu transmembrane domain and its involvement in the regulation of virus release from HIV-1-infected cells. FEBS Letters 398:12–18

Schwarz S, Wang K, Yu W, Sun B, Schwarz W (2011) Emodin inhibits current through SARS-associated coronavirus 3a protein. Antivir Res 90:64–69

Schwarz S, Sauter D, Lu W, Wang K, Sun B, Efferth T, Schwarz W (2012) Coronaviral ion channels as target for Chinese herbal medicine. Forum Immunopathol Dis Therap 3:1–13

Schwarz S, Sauter D, Wang K, Zhang RH, Sun B, Karioti A, Bilia AR, Efferth T, Schwarz W (2014) Kaempferol derivatives as antiviral drugs against 3a channel protein of coronavirus. Planta Med 80:177–182

Tu YY (2011) The discovery of artemisinin (qinghaosu) and gifts from Chinese medicine. Nature Medicine 17:1217–1220

Wang K, Xie S, Sun B (2011) Viral proteins function as ion channels. Biochim Biophys Acta 1808:510–515

Wu CH, Vasilets LA, Takeda K, Kawamura M, Schwarz W (2003) The N-terminus of the Na$^+$,K$^+$-ATPase α-subunit acts like an inactivation "ball". Biochim Biophys Acta 1609:55–62

Vasilets LA, Schwarz W (1993) Structure-function relationships of cation binding in the Na$^+$/K$^+$-ATPase. Biochim Biophys Acta 1154:201–222